

The onset of motion in a toroidal thermosyphon

Y. ZVIRIN

Faculty of Mechanical Engineering, TECHNION – Israel Institute of Technology, Haifa, Israel

(Received March 3, 1985 and in final form August 21, 1985)

Summary

The instability associated with the onset of motion in a toroidal natural-circulation loop has been studied theoretically. A one-dimensional model is used to investigate the problem of global flow initiation from a rest state. It is shown that a thermosyphonic flow is established when the modified Rayleigh number exceeds a critical value, R_c^* or R_c , which depends on the modified Biot number B . For a loop heated by a uniform heat flux R_c^* is between the limits of $\frac{1}{4}$ and 2.816 for small and large B , respectively. For a loop heated by a prescribed constant wall temperature, R_c has a minimal value of 2 at $B = 1$. These results were obtained by two methods: a direct solution of the steady-state problem and a stability analysis of the rest state. The latter shows that when $R^* > R_c^*$ there is a single monotonously growing perturbation and there are always additional monotonously decaying disturbance modes.

1. Introduction

Natural-circulation loops (thermosyphons) have recently gained increased interest; they appear in geophysical and engineering systems such as geothermal processes, solar heaters and nuclear-reactor cooling loops. Two recent reviews [1,2] include descriptions and discussions of practical applications, experimental and theoretical investigations of thermosyphons.

There are several instability modes exhibited in natural convection loops, as discussed in detail in [3]. The present work treats the instability associated with the onset of thermosyphonic motion from a rest state. It is noted that when the loop is not symmetric, i.e. the heating is supplied from the side, a flow would instantly be initiated upon applying the heat source. The onset of motion, then, is not defined as a stability problem. The loops in the energy-conversion systems mentioned above are mostly of this type.

Here we are concerned with the conditions determining the stability margin of the rest state of a symmetric loop. In this case the direction of the flow depends on the initial disturbance. There has been some controversy about the question whether a symmetric thermosyphon is always unstable with respect to the onset of motion. Pomerantsev [4] and Welander [5] investigated vertical closed loops with two parallel channels and a point heat source at the bottom. The former treated heat transfer from the fluid in the channels to the surroundings and the latter insulated branches and a point heat sink at the top. Both solved the steady-state problems and Welander also studied the stability of the steady flow. Both references [4 and 5] stated that the rest state (no-flow) in the loop is unstable for the whole range of system parameters. Their analyses, however, do not include thermal

conduction, which is a stabilizing effect. It is noted that Pomerantsev [4] included thermal conduction only in the boundary condition at the heat source, but neglected it in the solution procedure. Bau and Torrance [6] reached the same conclusion for an open thermosyphon. A zero perturbation-temperature gradient was imposed at the loop outlet, and in the case of adiabatic legs there is, then, no mechanism for disturbance damping. Heat conduction was considered in [6], but a linear distribution of the perturbation temperature was assumed. This assumption may lead to incorrect results as regards instabilities, cf. [7].

Other works have predicted critical conditions for the onset of motion in free-convection loops. Torrance and Chan [8] obtained a critical Rayleigh number for an open thermosyphon by an asymptotic expansion of the condition for a steady flow in the loop, without the explicit heat-conduction term in the energy equation.

Shaidurov [9] derived critical conditions for the onset of motion in a closed circuit by regarding the steady-state equations for small disturbances, including thermal diffusivity. The temperature perturbation was taken to be independent of the axial coordinate, and the analysis does not seem to treat a closed loop, which casts a serious doubt on the applicability of the results for thermosyphons.

Yorke and Yorke [10] and Hart [11] studied natural circulation in a toroidal loop. They have shown that in certain cases the structure of the flow in the loop is governed by a set of equations derived previously by Lorenz [12] for thermal convection between plane parallel plates. Lorenz showed from these equations that the rest state is stable when a modified Rayleigh number is below a certain limit, while above it a steady flow exists and the rest state is unstable. These results were applied in [10,11] to the toroidal loop, but they are restricted to some severe symmetry conditions on the driving forces of the loop (heating and cooling patterns). Moreover, these analyses do not include, again, the thermal conduction.

This assumption of negligible thermal diffusion is usually justified for steady flows or transients after a flow has already been initiated, and conduction becomes smaller compared to convection. In the stability analysis of the rest state, on the other hand, the stabilizing effect of heat conduction is important. Moreover, the thermal conduction term cannot be neglected in sections exposed to heating by a prescribed flux, because it is impossible to satisfy, then, the energy equation. In fact, heat conduction is the only mechanism of heat transfer in this case, as also pointed out in [6].

A recent analysis [3] (including thermal conduction) of the vertical loop similar to the one treated previously in [5], has revealed that there exists a critical Rayleigh number for the onset of motion. This result was obtained from the steady-state solution for the flow (which does not exist unless the Rayleigh number exceeds the critical value) and by a stability analysis of the rest state.

The present work deals with the toroidal thermosyphon, whose steady state and its stability have been extensively investigated, [10,11,13–18]. Similar to the results of [3], critical values are found for the Rayleigh number, associated with the onset of motion. These values depend on the Biot number, representing the cooling nature at the top half of the torus, while the bottom half is heated by a uniform heat flux. The stability margin is obtained from the steady-state solution and confirmed by a stability analysis of the rest state for two limiting cases: (a) the top (cooled) section of the loop is maintained at a constant temperature, (b) heat is evenly extracted at the upper section. It is shown that these cases correspond to high and low Biot numbers, respectively, and the results asymptotically approach those of the general solution for these limits.

Finally, an additional situation is treated (Section 3.2) where the heating at the bottom half is by prescribing a constant wall temperature. This case satisfies the symmetry conditions of [10,11]. It is shown, indeed, that their result can be derived from the general solution obtained here by an asymptotic expansion for small thermal conductivity.

2. The theoretical model

The toroidal loop, shown in Figure 1, is heated at the lower half by a constant heat flux q , and cooled from above by maintaining a constant wall temperature T_0 . Experiments on such a loop were reported in [15,16]. For the cooled section, a constant heat-convection coefficient h is assumed between the fluid and the wall, which may be considered as the average axial value. The formulation of the problem is actually more general: T_0 may represent a surroundings temperature and h an overall heat-transfer coefficient. Thus the results would also apply to cases where the external resistance to heat transfer is not negligible.

The onset of motion in the loop is investigated here; therefore the velocities are small and the flow is laminar. A two-dimensional analysis of this loop [13,14] indicates that the heat transfer and friction correlations approach, then, those for forced laminar flow in a tube: $Nu = 3.66$, $f = 16/Re$. These results justify the use of a one-dimensional model with W and T denoting cross-sectional average velocity and temperature. The Boussinesq approximation is used, i.e. the density ρ is considered to be constant in the governing equations except for the gravity term in the momentum equation, where $\rho = \rho_0[1 - \beta(T - T_0)]$, and β is the thermal expansion coefficient.

The continuity equation leads to the result that the velocity is a function of time only:

$$W = W(\tau). \quad (1)$$

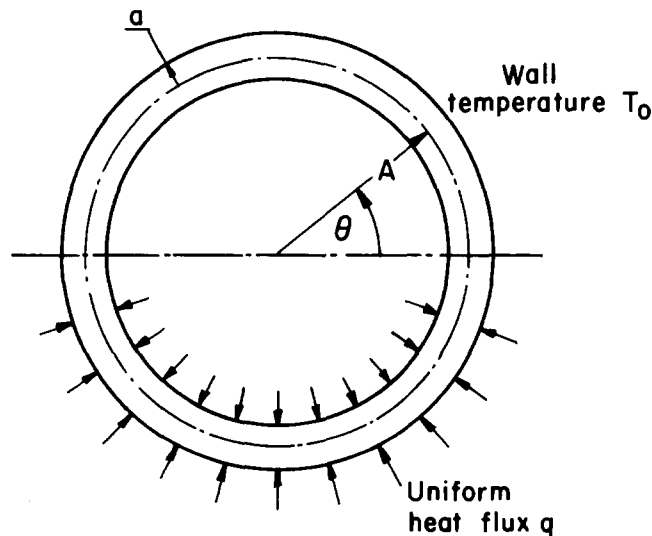


Figure 1. The geometry of the toroidal thermosyphon.

The momentum equation, integrated around the loop to eliminate the pressure term, and the energy equation are written in the following form, c.f. [15–17]:

$$\rho \frac{dW}{d\tau} = \frac{\rho\beta g}{2\pi} \int_0^{2\pi} T \cos \theta \, d\theta - \frac{8\mu W}{a^2}, \quad (2)$$

$$\rho c \left(\frac{\partial T}{\partial \tau} + \frac{W}{A} \frac{\partial T}{\partial \theta} \right) = \frac{k}{A^2} \frac{\partial^2 T}{\partial \theta^2} \begin{cases} -\frac{2h}{a} (T - T_0), & 0 \leq \theta \leq \pi, \\ +\frac{2q}{a}, & \pi \leq \theta \leq 2\pi, \end{cases} \quad (3a)$$

$$+ \frac{2q}{a}, \quad \pi \leq \theta \leq 2\pi, \quad (3b)$$

where a and A are the minor and major torus axes and θ is the axial coordinate (see Fig. 1); ρ is written instead of ρ_0 for brevity, g is the acceleration of gravity and μ , c and k are the dynamic viscosity, specific heat and thermal conductivity of the fluid. It is seen that the energy equation explicitly includes axial conduction, neglected in most of the previous thermosyphon analyses. Mertol [18] obtained a numerical solution for the toroidal loop taking into account this term, but he did not investigate the onset of motion, and his results do not include the limit of small W .

The boundary conditions for the energy equation are continuity of the temperature and its spatial derivative (heat flux) at the connections of the heated and cooled sections. They are written below in dimensionless form.

Equations (2,3) are transformed to the following dimensionless form:

$$\frac{1}{P} \frac{dw}{dt} = R^* \int_0^{2\pi} \phi \cos \theta \, d\theta - w, \quad (4)$$

$$\frac{\partial \phi}{\partial t} + w \frac{\partial \phi}{\partial \theta} = \frac{\partial^2 \phi}{\partial \theta^2} \begin{cases} -B\phi, & 0 \leq \theta \leq \pi, \\ +1, & \pi \leq \theta \leq 2\pi, \end{cases} \quad (5a)$$

$$+1, \quad \pi \leq \theta \leq 2\pi, \quad (5b)$$

where the non-dimensional time, velocity and temperature are defined by

$$t = \frac{\alpha}{A^2} \tau, \quad w = \frac{A}{\alpha} W, \quad \phi = \frac{ka}{2qA^2} (T - T_0). \quad (6)$$

The parameters appearing in eqs. (4,5) are the modified Rayleigh, Prandtl and Biot numbers:

$$R^* = \frac{\beta g q a A^3}{8\pi k \nu \alpha}, \quad P \equiv 8 \frac{\nu}{\alpha} \left(\frac{A}{a} \right)^2 = 8Pr \left(\frac{A}{a} \right)^2, \quad (7)$$

$$B \equiv \frac{2ha}{k} \left(\frac{A}{a} \right)^2 = 2Bi \left(\frac{A}{a} \right)^2$$

where α and ν are the thermal diffusivity and kinematic viscosity of the fluid.

As explained above, the boundary conditions for eqs. (5) are given by

$$\phi|_{\theta=0} = \phi|_{\theta=2\pi}, \quad \frac{\partial \phi}{\partial \theta} \Big|_{\theta=0} = \frac{\partial \phi}{\partial \theta} \Big|_{\theta=2\pi}, \quad (8a)$$

$$\phi|_{\theta=\pi^-} = \phi|_{\theta=\pi^+}, \quad \frac{\partial \phi}{\partial \theta} \Big|_{\theta=\pi^-} = \frac{\partial \phi}{\partial \theta} \Big|_{\theta=\pi^+}. \quad (8b)$$

3. Determination of the stability margin from the steady-state solution

As demonstrated in [3,10,11], the stability boundary associated with the onset of motion can be derived from the conditions for existence of a steady flow in the loop. This procedure is used in this section for finding the critical Rayleigh number for the onset of motion. The results are confirmed by a direct stability analysis for the limiting cases of high and low Biot number, see Section 4 and Appendices A and B.

3.1. Heating by a uniform heat flux at the bottom half

The steady-state problem is governed by eqs. (4) and (5) without the time derivatives and with the boundary conditions (8) for ϕ . The steady-state velocity w is constant around the loop. The energy equations (5) are therefore solved, first, for ϕ with w as a parameter. The solution is written in the following form:

$$\phi_U \equiv C_1 e^{\lambda_1 \theta} + C_2 e^{\lambda_2 \theta}, \quad 0 \leq \theta \leq \pi, \quad (9a)$$

$$\phi_L = C_3 e^{w\theta} + C_4 + \frac{\theta}{w}, \quad \pi \leq \theta \leq 2\pi, \quad (9b)$$

where

$$\lambda_{1,2} = \frac{w}{2} \left[1 \pm \left(1 + \frac{4B}{w^2} \right)^{1/2} \right]. \quad (10)$$

Introducing the temperature distributions (9) into the boundary conditions (8), the following relations are obtained for the constants of integration C_i :

$$C_1 + C_2 - C_3 e^{2\pi w} - C_4 = \frac{2\pi}{w}, \quad (11a)$$

$$C_1 e^{\pi\lambda_1} + C_2 e^{\pi\lambda_2} - C_3 e^{\pi w} - C_4 = \frac{\pi}{w}, \quad (11b)$$

$$C_1 \lambda_1 + C_2 \lambda_2 - C_3 w e^{2\pi w} = \frac{1}{w}, \quad (11c)$$

$$C_1 \lambda_1 e^{\pi\lambda_1} + C_2 \lambda_2 e^{\pi\lambda_2} - C_3 w e^{\pi w} = \frac{1}{w}. \quad (11d)$$

This is a set of four equations for the four unknowns C_i , $i = 1, \dots, 4$. It is possible to obtain explicit expressions for C_i ; however, a numerical solution must be performed for the general case (see below). It is therefore more convenient to find the constants C_i directly from eqs. (11) by the numerical algorithm.

The temperature distributions (9) are introduced now into the momentum equation (4). Evaluating the temperature integral, we obtain

$$\begin{aligned} Z(w; B) &= \int_0^{2\pi} \phi \cos \theta \, d\theta \\ &= -C_1 \frac{\lambda_1(1 + e^{\pi\lambda_1})}{1 + \lambda_1^2} - C_2 \frac{\lambda_2(1 + e^{\pi\lambda_2})}{1 + \lambda_2^2} + C_3 \frac{w e^{\pi w}(1 + e^{\pi w})}{1 + w^2} + \frac{2}{w}. \end{aligned} \quad (12)$$

Eq. (4) for the steady state reduces now to the form

$$R^* = \frac{w}{Z(w; B)} \quad (13)$$

which is a non-linear algebraic equation for the velocity w depending on the modified Rayleigh and Biot numbers R^* and B (note that the constants C_i depend only on w and B , eqs. (11), (10)).

As mentioned above, a numerical method must be employed for solving eq. (13). The solution procedure can be significantly simplified by calculating $R^*(w)$ for various values of B , rather than attempting a direct computation of w . It is noted that $R^*(w)$ should be a monotonously increasing function in the range $w > 0$, because a stronger driving force would produce a higher velocity. Also, the problem is symmetric and therefore, for any value of the steady-state velocity w , $-w$ is a solution too. These properties have been observed, indeed, from the numerical results, and they are also depicted by the expressions for the limiting cases, eqs. (A-5) and (B-3).

The numerical algorithm first calculates the constants C_i from eqs. (11) and then finds $R^*(w; B)$ from eqs. (12,13). Figure 2 shows the results for the steady-state velocity w as a function of the modified Rayleigh number R^* for various values of the Biot number B . It can be seen that the numerical results approach the analytical solutions for small and large B (Appendices A and B): the former at $B = 0.1$ and the latter at $B > 1000$.

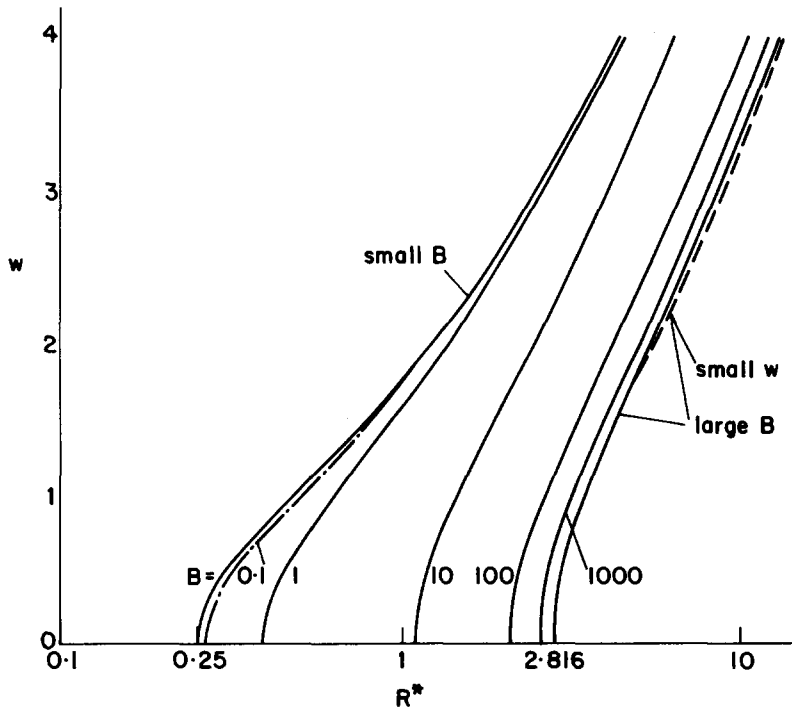


Figure 2. The dimensionless steady-state velocity w as a function of the modified Rayleigh and Biot numbers, R^* and B .

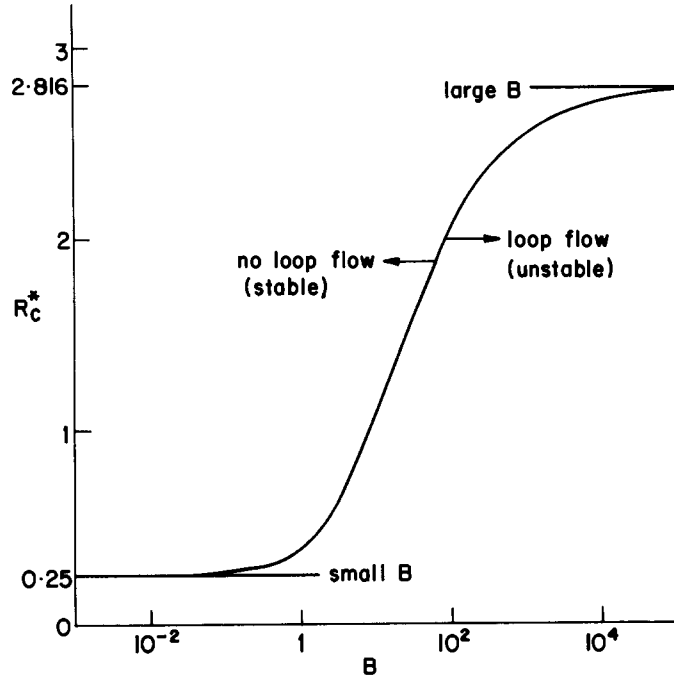


Figure 3. The critical modified Rayleigh number R_c^* as a function of the modified Biot number B . Heating by a constant heat flux.

Before presenting the results pertaining to the stability associated with the onset of motion, let us discuss some general results for the steady flow in the loop. It is first noted that the steady-state behavior is governed by the two parameters R^* and B . Metol [18] used different scaling and presented his results by different dimensionless parameters. A comparison of the formal presentations shows that the values of the non-dimensional velocities ($w_{s,s}$) of [18] must be multiplied by $2R^{*1/2}$ in order to arrive at the values of w in the present work. The numerical results obtained here exactly match, indeed, those of [18].

For large values of R^* the steady-state velocity w increases and axial conduction becomes negligible with respect to the convection. The results of the numerical method and the analytical solutions in the Appendices completely agree with previous studies which did not take into account the conduction term. In this case the steady-state solution depends on a single parameter, denoted by D in [17]. It can be shown that $D = \pi B / (2R^{*1/2})$. For $B \ll 1$ the analytical solution (Appendix B) yields $w = 2R^{*1/2}$ and $W = W_{ch} = \{\beta g q A a / (2\pi c \mu)\}^{1/2}$. This is the result obtained in [15–17] for small D . For $B \gg 1$, the analytical solution (Appendix A) leads to $w = (2R^*)^{1/2}$, or $W = W_{ch} / 2^{1/2}$, agreeing with [17]. For intermediate values of B the numerical solution agrees, again, with the results of [17].

The results in Fig. 2 show that for any value of B there exists a critical value R_c^* of the Rayleigh number below which there does not exist a steady-state solution. $R_c^*(B)$ was found by letting $w \rightarrow 0$ in the numerical calculations. This stability boundary for the onset of motion is shown in Fig. 3. The figure also includes the limits for small and large B ,

obtained in the Appendices, $R_c^* = \frac{1}{4}$ and 2.816, respectively. A further discussion of the results appears in Section 5.

3.2. Heating by a prescribed wall temperature at the bottom half

Let us now consider the case where the loop is heated by maintaining a prescribed wall (or surroundings) temperature, $T_0 + \Delta T$, at the lower half instead of a uniform heat flux. This situation satisfies the symmetry conditions of [10,11]: the “driving heating function”, i.e. the wall temperature, is symmetric with respect to the vertical loop axis ($\theta = \frac{1}{2}\pi, \frac{3}{2}\pi$), and antisymmetric with respect to the horizontal axis ($\theta = 0, \pi$) about the mean temperature $T_0 + \frac{1}{2}\Delta T$.

The mathematical formulation of the problem is that of Section 2, with a change only in the energy equation for the bottom half, $\pi \leq \theta \leq 2\pi$, where the second term on the RHS of eq. (3b) is now $(2h/a)[(T_0 + \Delta T) - T]$. The dimensionless temperature is defined by $\phi = (T - T_0)/\Delta T$ and the Rayleigh number $R = \beta g \Delta T a^2 A / (16\pi\nu\alpha)$ appears now in the momentum equation (4) instead of R^* . The dimensionless energy equation for the upper half (5a) remains unchanged while for the lower half the term $B(1 - \phi)$ replaces the second term on the RHS of eq. (5b). The other parameters in eqs. (6), (7) and the boundary conditions (8) retain their form.

The solution procedure is similar to that of Section 3.1. The energy equations (5) are first solved with the velocity w as a constant parameter, yet unknown:

$$\phi_U = D_1 e^{\lambda_1\theta} + D_2 e^{\lambda_2\theta}, \quad 0 \leq \theta \leq \pi, \quad (14a)$$

$$\phi_L = D_3 e^{\lambda_1\theta} + D_4 e^{\lambda_2\theta} + 1, \quad \pi \leq \theta \leq 2\pi, \quad (14b)$$

where $\lambda_{1,2}$ are given in Eq. (10) and the constants of integration D_i are found from the boundary conditions (8). Introduction of the results into the momentum equation (4) and performing the temperature integral, an algebraic equation is obtained for the velocity w whose solution is

$$w = \left[2BR - (1 + B)^2 \right]^{1/2}. \quad (15)$$

This solution shows that there exists a condition for a steady flow in the loop, namely,

$$R > R_c = (1 + B)^2 / 2B. \quad (16)$$

The critical Rayleigh number $R_c(B)$ for this case is shown in Fig. 4. The figure also includes the approximation $R_c = \frac{1}{2}B$ for large B . When the thermal-conduction influence is small, both B and R become large and the results approach those of [11], where heat conduction was neglected: it can be shown that the parameter Ra of [11] (which does not include k or α) is equal to $2R/B$ and in the limit of large B and R the rest state becomes unstable at $Ra = 1$, as concluded in [11]. Moreover, the dimensionless velocity in terms of the notation of [11] is $w/B = \pm (Ra - 1)^{1/2}$, which is the asymptotic approximation of the present solution (15) for large B and R .

The conduction (or diffusion) of heat is a stabilizing effect. Figure 4 shows, indeed, that the neglect of the relevant terms leads to a lower stability margin. The approximation for

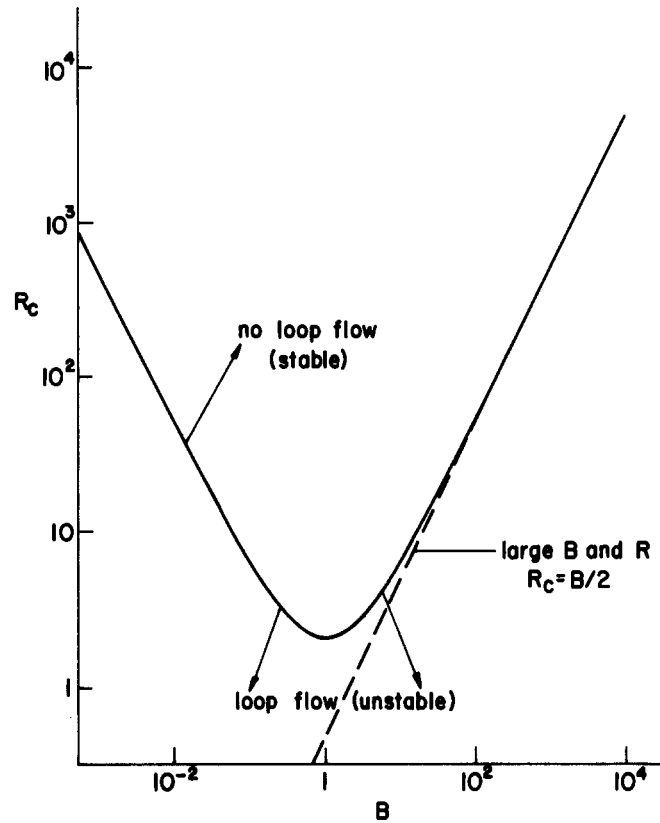


Figure 4. The critical modified Rayleigh number R_c as a function of the modified Biot number B . Heating by a prescribed constant wall temperature.

large B (which may be interpreted as small conductivity) is valid for $B > \sim 20$. The results are discussed further in Section 5.

4. Stability of the rest state

The critical Rayleigh number for the initiation of flow in the loop was derived in the previous section on the basis of the steady-state solution. The instability associated with the onset of motion is treated in this section. For this, the temperature distribution $\bar{\phi}(\theta)$ in the steady rest state (no flow) is first obtained from eqs. (5,8) with $w = 0$. It is then assumed that the time-dependent velocity and temperature can be expressed by

$$w = u e^{\sigma t}, \quad \phi = \bar{\phi} + \psi(\theta) e^{\sigma t}, \quad (17)$$

where u and ψ are small perturbations (the continuity equation implies that u is constant), and σ is the stability parameter. The condition for stability is $\text{Real}(\sigma) < 0$. Linear stability analysis is used, whereby the distributions (17) are introduced into the governing equations (4,5) and boundary conditions (8). The steady- (rest-) state terms

identically cancel and second-order terms are neglected. The perturbation energy and momentum equations obtained in this way are

$$\sigma\psi + u\frac{\partial\bar{\phi}}{\partial\theta} = \frac{\partial^2\psi}{\partial\theta^2} \begin{cases} -B\psi, & 0 \leq \theta \leq \pi, \\ +0, & \pi \leq \theta \leq 2\pi, \end{cases} \quad (18a)$$

$$(18b)$$

$$u\left(1 + \frac{\sigma}{P}\right) = R^* \int_0^{2\pi} \psi \cos \theta \, d\theta. \quad (19)$$

The boundary conditions for ψ have the same form as eqs. (8). Solving eqs. (18) for ψ in terms of u , introducing the result into (19) and eliminating u , an algebraic characteristic equation for σ is obtained. The stability analysis was performed separately for the limiting cases of large and small B (their steady-state solutions appear in the Appendices). It is noted that in these cases the governing equations do not include the parameter B . The solutions are, therefore, independent of any assumption on the heat-transfer correlation for h .

4.1. Large Biot number, $B \gg 1$

In this case the temperature at the cooled section of the torus is constant, $\phi = 0$, and therefore also $\bar{\phi} = 0, \psi = 0$. The solution of the energy equation (5b) for the steady rest state is

$$\bar{\phi}_L = -\frac{1}{2}\theta^2 + \frac{3}{2}\pi\theta - \pi^2, \quad \pi \leq \theta \leq 2\pi, \quad (20)$$

which satisfies the boundary conditions $\bar{\phi}|_0 = \bar{\phi}|_{2\pi} = 0$. This expression is introduced into eq. (18b), and the solution for ψ , satisfying the conditions $\psi|_0 = \psi|_{2\pi} = 0$, is given by

$$\psi_L = u \left[G_1 e^{\gamma\theta} + G_2 e^{-\gamma\theta} + \frac{1}{\sigma} \left(\theta - \frac{3}{2}\pi \right) \right], \quad \pi \leq \theta \leq 2\pi, \quad (21)$$

where

$$G_1 = -\frac{\pi}{2\sigma} \frac{e^{-\pi\gamma} + 1}{e^{2\pi\gamma} - 1}, \quad G_2 = \frac{\pi}{2\sigma} \frac{e^{\pi\gamma} + 1}{e^{2\pi\gamma} - 1} e^{2\pi\gamma}, \quad \gamma = \sqrt{\sigma}. \quad (22)$$

The perturbation-temperature distribution (21) is substituted into the momentum equation (19). Performing the integral and eliminating u , the following characteristic equation for σ is obtained:

$$1 + \frac{\sigma}{P} = \frac{R^*}{\sigma} \left[2 - \frac{\pi\gamma}{1 + \gamma^2} \frac{e^{\pi\gamma} + 1}{e^{\pi\gamma} - 1} \right]. \quad (23)$$

In general, eq. (23) must be solved numerically for $\sigma(R^*, P)$. The main interest here, however, is the investigation of the behavior near the critical value of the modified Rayleigh number, $R_c^* = 2.816$, obtained for this case in Section 3.1 and Appendix A (eq.

A-7). An expansion of eq. (23) for small values of σ and γ (it is necessary to retain fifth-order terms, as in the steady-state solution, Appendix A), yields:

$$\gamma = \pm \left[\frac{\frac{R^*}{R_c^*} - 1}{1 + \frac{\pi^2}{6} + \frac{1}{P} - R_c^* \pi^2 \left(\frac{1}{3} - \frac{\pi^2}{40} \right)} \right]^{1/2}, \quad \left| \frac{R^*}{R_c^*} - 1 \right| \ll 1. \quad (24)$$

When $R^* > R_c^*$, γ is real and σ is positive, see Eq. (22); for $R^* < R_c^*$, γ is imaginary and σ is negative (the denominator in eq. (24) is always positive). In both cases eqs. (24) and (22) lead to

$$\sigma = \frac{\frac{R^*}{R_c^*} - 1}{1 + \frac{1}{6}\pi^2 + \frac{1}{P} - R_c^* \pi^2 \left(\frac{1}{3} - \frac{1}{40}\pi^2 \right)}, \quad \left| \frac{R^*}{R_c^*} - 1 \right| \ll 1. \quad (25)$$

This result shows that when the Rayleigh number is just below the critical value $R_c^* = 2.816$, a disturbance to the rest state decays monotonously and no steady flow would be established. When $R^* > R_c^*$, the rest state is unstable and a perturbation would increase monotonously to approach the steady-state solution.

Eq. (23) does not have any complex roots; therefore, there exist no oscillatory perturbation modes. There are, however, multiple real roots σ for every R^* and P , all of which are negative except for the case $R^* > R_c^*$ where there also exists a single positive solution. For $\sigma < 0$, eq. (23) can be transformed to

$$R^* = \frac{\sigma(1 + \sigma/P)}{2 + \frac{\pi\delta}{\delta^2 - 1} \cot(\frac{1}{2}\pi\delta)}, \quad \delta = \sqrt{-\sigma}, \quad \sigma < 0, \quad (26)$$

which is a transcendental equation for σ with an infinite number of negative roots, indicating numerous decaying disturbance modes.

Figure 5 shows the numerical solution of eq. (23) for the largest root of the stability parameter σ as a function of the modified Rayleigh number R^* for various values of the modified Prandtl number P . The asymptotic behavior near $R^* = R_c^*$ (eq. 25) is also illustrated in Fig. 5b as well as the limiting solution of eq. (23) for large R^* , $\sigma = (2PR^*)^{1/2}$.

4.2. Small Biot number, $B \ll 1$

When the Biot number is small the heat flux at the cooled upper part approaches a constant value whose absolute value is q , as explained in Appendix B. The energy equations for this case are (5b) and (B-4) replacing (5a), with the boundary conditions (8) and the additional arbitrary condition $\sigma|_0 = \phi|_{2\pi} = 0$. The solution for the steady rest

* In Appendix B another value is chosen, for convenience, for $\phi|_0 = \phi|_{2\pi}$ without losing generality.

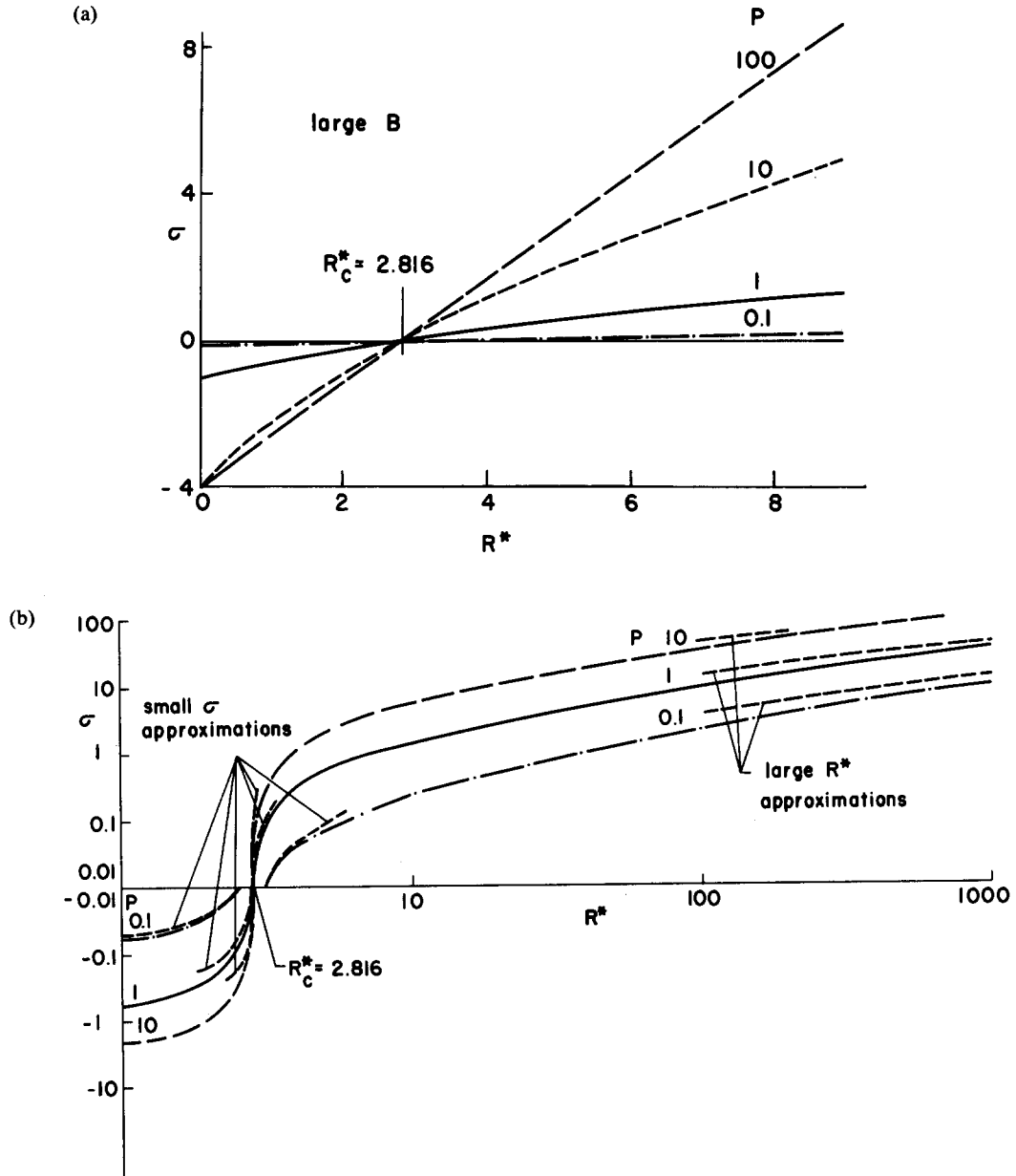


Figure 5. The largest root of the stability parameter σ as a function of the modified Rayleigh and Prandtl numbers, R^* and P , for large values of the Biot number B . (a) the range $0 \leq R^* \leq 8$, (b) the range $0.1 \leq R^* \leq 1000$.

state ($\partial\phi/\partial t = 0$, $w = 0$) is given by

$$\bar{\phi}_U = \frac{1}{2}\theta^2 - \frac{1}{2}\pi\theta, \quad 0 \leq \theta \leq \pi, \quad (27a)$$

$$\bar{\phi}_L = -\frac{1}{2}\theta^2 + \frac{3}{2}\pi\theta - \pi^2, \quad \pi \leq \theta \leq 2\pi. \quad (27b)$$

These expressions are introduced into the perturbed energy equations (18), with a zero

replacing the term $B\psi$ in (18a). The solution for the temperature disturbances is written as

$$\psi_U = u \left[H_1 e^{\gamma\theta} + H_2 e^{-\gamma\theta} + \frac{1}{\sigma} \left(-\theta + \frac{1}{2}\pi \right) \right], \quad 0 \leq \theta \leq \pi, \quad (28a)$$

$$\psi_L = u \left[H_3 e^{\gamma\theta} + H_4 e^{-\gamma\theta} + \frac{1}{\sigma} \left(\theta - \frac{3}{2}\pi \right) \right], \quad \pi \leq \theta \leq 2\pi, \quad (28b)$$

where the constants of integration H are found from the boundary conditions for ψ , having the same form as eqs. (8),

$$H_1 = \frac{1}{\gamma^3} \frac{1 - e^{\pi\gamma}}{1 - e^{2\pi\gamma}}, \quad H_2 = -\frac{1}{\gamma^3} \frac{e^{\pi\gamma}(1 - e^{\pi\gamma})}{1 - e^{2\pi\gamma}}, \quad (29a)$$

$$H_3 = \frac{1}{\gamma^3} \frac{1 - e^{-\pi\gamma}}{1 - e^{2\pi\gamma}}, \quad H_4 = \frac{1}{\gamma^3} \frac{1 - e^{\pi\gamma}}{1 - e^{2\pi\gamma}} e^{2\pi\gamma}, \quad (29b)$$

$$\gamma = \sqrt{\sigma}. \quad (29c)$$

The perturbation temperature distribution (28) is introduced into the momentum

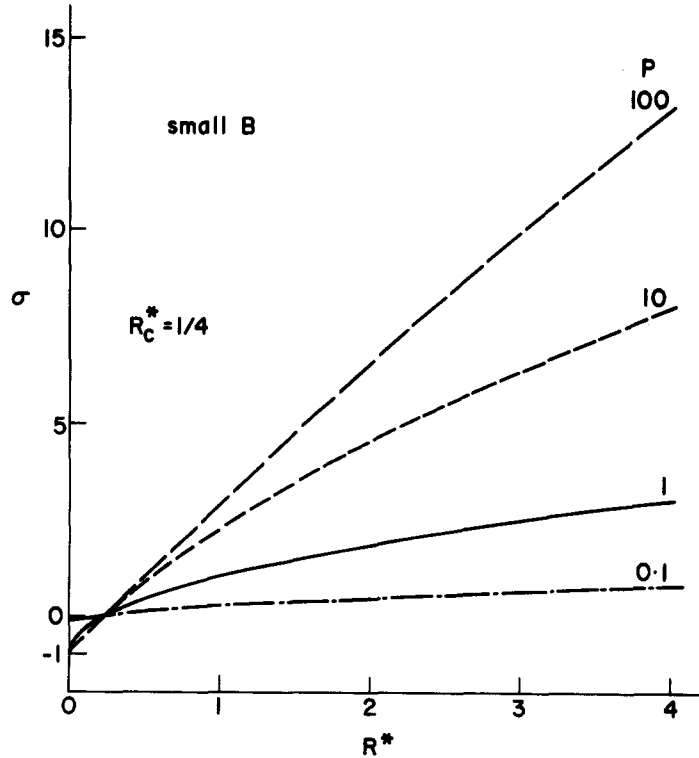


Figure 6. The largest root of the stability parameter σ as a function of the modified Rayleigh and Prandtl numbers, R^* and P , for small values of the Biot number B .

equation (19). Carrying out the integration and eliminating u lead to the following characteristic equation for the stability parameter σ :

$$1 + \frac{\sigma}{P} = \frac{4R^*}{1 + \sigma}. \quad (30)$$

This is a simple quadratic equation, whose solution is

$$\sigma = \frac{1}{2} \left\{ -(P + 1) \pm \left[(P - 1)^2 + 16PR^* \right]^{1/2} \right\}. \quad (31)$$

As can be seen, when $R^* > R_c^* = \frac{1}{4}$ for this case, there is always (for any value of P) a positive real root for σ . This confirms the result derived in Appendix B, that the condition for the onset of motion is determined by this critical value of the modified Rayleigh number, R_c^* . For $R^* > R_c^*$ there would always exist a monotonously increasing disturbance, and for $R^* < R_c^*$ the rest state is stable: any perturbation would monotonously decay, because σ has two negative real roots. It is noted that since P and R^* are both positive, the expression under the square root of eq. (31) is always positive and all the roots are real, so that no oscillatory modes exist. The solution for the largest root σ for this case of small B is shown in Figure 6.

5. Discussion

The stability associated with the onset of motion in a toroidal thermosyphon has been investigated by two methods: (a) derivation of a steady-state solution for the flow in the loop and determination of the condition for its existence, (b) direct stability analysis of the rest (no-flow) state. The results show that there exists a critical value of the modified Rayleigh number which depends on the modified Biot number.

Figure 3 shows the marginal stability chart of the rest state for a loop heated by a uniform heat flux. The critical modified Rayleigh number R_c^* increases with B from the value $\frac{1}{4}$, which is the limit for small B , to 2.816 for large B . As B increases, the fluid temperature in the cooled upper half decreases axially (with θ) more strongly and approaches the wall temperature, i.e. a symmetric distribution with respect to the vertical axis. (In the limit the temperature becomes uniform and equal to T_0 , see Appendix A). The net buoyancy driving force is therefore reduced, and the loop is more stable.

The stability margin for the rest state of a loop heated by a prescribed temperature is illustrated in Fig. 4. The asymptotic expansion for large B and R is also shown (lower line), which demonstrates the stabilizing effect of the thermal diffusion. For $B > 1$ the rest state becomes more stable as B increases, as demonstrated above. However, the loop in this case is also more stable (as regards the onset of motion) when B decreases ($B < 1$). This phenomenon can be explained by the behavior for $B \rightarrow 0$: the fluid, then, is less heated by the heat source and the mechanism driving the flow becomes weaker.

It is interesting to look at some typical values corresponding to Creveling's experiments [15]. The torus, with $A = 38$ cm and $a = 1.5$ cm, was filled with water. At a heat-flux input of 2000 w/m² the average water temperature was 31°C and the estimated mean value of h based on $Nu = 3.66$ (see Section 2) is 74 w/m² °C. These data lead to: $R^* = 2.9 \times 10^9$, $P = 3.1 \times 10^4$ and $B = 2.3 \times 10^3$. Obviously, this situation is unstable as regards the onset of motions, see Fig. 3. All the tests in this loop were at very high Rayleigh numbers and a

global flow was always established. It would be possible to approach the stability boundary in a loop of a much smaller scale, at a lower heat input and with a different fluid, having either a higher viscosity (e.g. glycerol) or a higher thermal conductivity (e.g. liquid metal).

Appendix A. Large Biot number, $B \gg 1$

When the modified Biot number B is large, the temperature of the cooled upper section of the torus sharply decreases with θ near the entrance ($\theta = 0$) and rapidly reaches the wall temperature T_0 . As a limiting case, therefore, we can take

$$\phi = 0, \quad 0 \leq \theta \leq \pi, \quad (\text{A-1})$$

instead of eq. (5a), see also eq. (6). The momentum equation (4) and the energy equation (5b) remain unchanged for the case of heating by a constant heat flux. The boundary conditions to be satisfied are continuity of the temperature only in eqs. (8).

The method of solution for the steady flow is similar to that described in Section 3. Eq. (5) is first solved for ϕ with w as a constant parameter, unknown at this stage:

$$\phi = E_1 e^{w\theta} + E_2 + \frac{\theta}{w}, \quad \pi \leq \theta \leq 2\pi. \quad (\text{A-2})$$

The constants of integration $E_{1,2}$ are found from the boundary conditions $\phi = 0$ at $\theta = \pi, 2\pi$:

$$E_1 = -\frac{\pi e^{-2\pi w}}{w(1 - e^{-\pi w})}, \quad E_2 = -E_1 e^{\pi w} - \frac{\pi}{w}. \quad (\text{A-3})$$

The integral in the momentum equation (4) is performed using the distributions (A-1), (A-2), to yield

$$Z(w) = \int_0^{2\pi} \phi \cos \theta \, d\theta = \frac{E_1 w e^{2\pi w}}{1 + w^2} (1 + e^{-\pi w}) + \frac{2}{w}. \quad (\text{A-4})$$

Introducing this function into eq. (4) we get the following algebraic equation for the steady-state velocity:

$$R^* \left[\frac{2}{w} - \frac{\pi(1 + e^{-\pi w})}{(1 + w^2)(1 - e^{-\pi w})} \right] = w. \quad (\text{A-5})$$

The solution, obtained by computing $R^*(w)$ as explained in Section 3, is illustrated in Fig. 2. The general numerical results presented in the figure approaches this solution when $B \gg 1$.

The critical Rayleigh number R_c^* and the behavior of the loop in its neighborhood can be found analytically from a careful expansion* of eq. (A-5), leading to the expression

$$w = \pm \left[\frac{R^*(2 - \frac{1}{6}\pi^2) - 1}{(1 + \frac{1}{6}\pi^2) - R^*\pi^2(\frac{1}{3} - \frac{1}{40}\pi^2)} \right]^{1/2}, \quad w \ll 1, \quad (\text{A-6})$$

* The leading-term approximation (A-6) has been derived by fifth-order expansions, similar to [3].

The last relationship yields the following critical value for the modified Rayleigh number:

$$R_c^* = \frac{1}{2 - \frac{1}{6}\pi^2} = 2.816, \quad (\text{A-7})$$

and eq. (A-6) can be reduced to

$$w = \pm \left\{ \frac{R^* - R_c^*}{R_c^* \left[1 - \frac{\pi^4}{60(12 - \pi^2)} \right]} \right\}^{1/2}. \quad (\text{A-8})$$

Eqs. (A-6) and (A-8) clearly show that there is no steady-state solution (no flow) when $R^* < R_c^*$. Figure 2 includes the analytical approximation (A-8) for large B . As can be seen, it is very close to the exact numerical solution for the whole range covered in the figure ($w < 4$), and not only for $w \ll 1$.

Appendix B. Small Biot number, $B \ll 1$

The limiting case of a loop heated from below by a constant heat flux and cooled by a constant wall temperature with a small Biot number at the top half can be solved by expanding the steady-state results of Section 3.1. For $B \ll 1$, eq. (10) yields

$$\lambda_1 = w + B/w + O(B^2), \quad \lambda_2 = -B/w + O(B^2). \quad (\text{B-1})$$

The constants of integration C_i are obtained from eqs. (11), and the temperature distributions (eqs. 9) take the form

$$\phi_U = \frac{1}{B} + \frac{2}{w^2(1 + e^{\pi w})} e^{w\theta} - \frac{\theta}{w}, \quad 0 \leq \theta \leq \pi, \quad (\text{B-2a})$$

$$\phi_L = \frac{1}{B} - \frac{2}{w^2 e^{\pi w}(1 + e^{\pi w})} e^{w\theta} + \frac{\theta}{w} + \frac{2}{w^2} - \frac{2\pi}{w}, \quad \pi \leq \theta \leq 2\pi. \quad (\text{B-2b})$$

Introducing these expressions into the momentum equation (4) (or using eqs. (12,13)), an algebraic equation for the velocity w is obtained whose solution is:

$$w = (4R^* - 1)^{1/2}. \quad (\text{B-3})$$

The critical value of the modified Rayleigh number for this case is obviously $R_c^* = \frac{1}{4}$. Figure 2 includes the result (B-3) as the limit for small B . Numerical results (Section 3) for $B = 0.1$ are quite close to this limit.

It will be shown now that, in the limit of small Biot number, the cooling nature at the upper half of the torus approaches that of uniform heat withdrawal. At steady state, then, the heat flux there will have the same absolute value, q , of the heat-flux input in the lower half. This case was solved in [16] (without axial conduction). The governing momentum

and energy equations (4,5b) and the boundary conditions (8) remain unchanged, while the energy equation for the cooled section, (5a), is replaced by

$$\frac{\partial \phi}{\partial t} + w \frac{\partial \phi}{\partial \theta} = \frac{\partial^2 \phi}{\partial \theta^2} - 1, \quad 0 \leq \theta \leq \pi. \quad (\text{B-4})$$

It is noted that neither the governing equations nor the boundary conditions explicitly include any reference temperature. We can therefore choose arbitrarily:

$$\phi|_0 = \phi|_{2\pi} = \frac{1}{B} + \frac{2}{w^2(1 + e^{\pi w})}, \quad (\text{B-5})$$

so as to match the temperature value at this point with the solution (B-2) for small B . Solving eqs. (5a) and (B-4) with the conditions (8) and (B-5), we get exactly the temperature distributions (B-2) and therefore also the velocity w from Eq. (B-3).

The approximation for small B cannot be extended to $B=0$ because there is no mechanism, then, for steady heat removal from the system. The solution (B-2) indicates indeed that the steady-state temperature rises as $1/B$ when B becomes very small. At the same time, when B is diminished, the fluid temperature in the cooled section decreases more slowly with θ , causing a stronger asymmetry of the buoyancy forces and thus a higher velocity – see also Fig. 2. The temperature difference $\phi|_{2\pi} - \phi|_{\pi}$ over the heated section decreases, then, as can be observed from a simple heat balance. The result is that the relative variation of the temperature becomes very small ($\Delta\phi$ decreases and ϕ increases). Therefore, the term $-B\phi$ in the RHS of eq. (5b) approaches -1 in the limit of small B , which corresponds to a uniform heat removal.

References

- [1] Y. Zvirin, A review of natural circulation loops in pressurized water reactors and other systems, *Nuclear Eng. Des.* 67 (1981) 203–225.
- [2] A. Mertol and R. Greif, A review of natural circulation loops, *NATO Advanced Study Inst. on Natural Convection*, Izmir, Turkey, July 16–27 (1984). Also in: *Natural Convection: Fundamentals and Applications*, Eds. W. Aung, S. Kakac and R. Viskanta, Hemisphere Publishing Corp., New York (1985).
- [3] Y. Zvirin, The instability associated with the onset of motion in a thermosyphon, *Int. J. Heat Mass Transfer* 28 (1985) 2105–2111.
- [4] A.A. Pomerantsev, An accurate theory of free convection, *Inzh. Fiz. Zh.* 4(6) (1961) 21–26.
- [5] P. Welander, On the oscillatory instability of a differentially heated fluid loop, *J. Fluid Mech.* 29 (1966) 17–30.
- [6] H.H. Bau and K.E. Torrance, Transient and steady behavior of an open symmetrically-heated free convection loop, *Int. J. Heat Mass Transfer* 24 (1981) 597–609.
- [7] Y. Zvirin and R. Greif, Transient behavior of natural circulation loops; two vertical branches with point heat source and sink, *Int. J. Heat Mass Transfer* 22 (1979) 499–504.
- [8] K.E. Torrance and V.W.L. Chan, Heat transfer by a free-convection loop embedded in a heat conducting solid, *Int. J. Heat Mass Transfer* 23 (1980) 1091–1097.
- [9] G.F. Shaidurov, Convective liquid stability in closed circuits, *Int. J. Heat Mass Transfer* 11 (1968) 235–239.
- [10] J.A. Yorke and E.D. Yorke, Chaotic behavior and fluid dynamics, in: *Topics in Applied Physics, Hydrodynamic Instabilities and the Transition to Turbulence*, edited by H.L. Swinney and J.P. Gollub, Springer-Verlag, Berlin (1981), Ch. 4.
- [11] J.E. Hart, A new analysis of the closed loop thermosyphon, *Int. J. Heat Mass Transfer* 27 (1984) 125–136.
- [12] E.N. Lorenz, Deterministic nonperiodic flow, *J. Atmos. Sci.* 20 (1963) 130–141.

- [13] A. Mertol, R. Greif and Y. Zvirin, Two dimensional study of heat transfer and fluid flow in a natural convection loop, *J. of Heat Transfer* 104 (1982) 508–514.
- [14] A. Ronen and Y. Zvirin, The behavior of a toroidal thermosyphon at high-Graetz (and Grashof) numbers, *J. Heat Transfer* 107 (1985) 254–258.
- [15] H.F. Creveling, J.F. DePaz, J.Y. Baladi and R.J. Schoenhals, Stability characteristics of a single-phase free convection loop, *J. Fluid Mech.* 67 (1975) 65–84.
- [16] P.S. Damerell and R.J. Schoenhals, Flow in a toroidal thermosyphon with angular displacement of heated and cooled sections, *J. Heat Transfer* 101 (1979) 672–676.
- [17] Y. Zvirin, The effect of dissipation on free convection loops, *Int. J. Heat Mass Transfer* 22 (1979) 1539–1546.
- [18] A. Mertol, Heat transfer and fluid flow in thermosyphons, Ph.D. Thesis, Dept. of Mech. Eng., University of California, Berkeley (1980).